コントロール：*PMP22*発現抑制物質のスクリーニングなど、2）変異アレルの発現抑制：siRNA、deoxribozymes、Antisense oligonucleotides（ASO）、RNA trans-splicingアプローチなど、3）欠損遺伝子・蛋白の補充：欠失している遺伝子の導入、既存薬の応用、4）凝集体形成抑制：凝集体形成や蛋白折りたたみ異常の阻害物質の探索などが期待される[7]（表）。

CMT患者が他の内科疾患等に罹患した場合に使用される薬剤が末梢神経障害を悪化させる場合がある。特にビンクリスチンなどがCMTの症状を悪化させる薬剤として有名である（http://www.charcot-marie-tooth.org/med_alert.php）。最近、癌化学治療薬の投与により末梢神経障害が顕在化し、CMTの遺伝子変異が明らかとなった例が報告されている。CMTの臨床症状を示さない潜在的なCMT患者がいる可能性があり、抗腫瘍薬（ビンクリスチンなど）投与前の神経伝導検査の実施は、末梢神経障害の重症化を防ぐ点で可能な限り推奨される。神経伝導検査と遺伝子検査を組み合わせることで、より安全・安心な癌化学療法が可能となりうる。

CMTの外科的治療

関節変形が進行し、装具を用いても足を適切な位置に保てず歩行に支障が出てきた場合、関節の安定性を図るために腱延長術や骨切り術などの整形外科手術が適応となる場合がある。外科治療が一般的に長期的な効果を有するかどうかについては現時点では十分なエビデンスはない。外科手術の長所と短所をCMT患者、家族と十分に検討した上で施行することが重要である。

手術適応：骨・関節の変形による痛みが強い場合、変形や筋力低下により歩行障害や日常生活での支障が著しい場合、変形により皮膚に潰瘍ができた場合などがCMTに対する手術適応となる。

手術方法：足に対する手術が最も多い。尖足・下垂足に対して、アキレス腱延長術、筋腱移行術が行われる。アキレス腱延長術（Sliding lengthening法）では、3か所でアキレス腱を横切し、足関節を背屈強制することでアキレス腱を延長する。この方法では腱縫合は不要である。後脛骨筋腱移行術は後脛骨筋腱を前方へ移行することで下垂した足をつり上げる。

表. Charcot-Marie-Tooth病（CMT）の治療法の開発
CMTの遺伝子診断を踏まえて以下のような事項がCMTの治療法開発に必要である。

1）CMTの病型別自然経過の解明
疾患頻度が低いCMT病型も多く、その自然経過を明きからにするためには国際共同研究が必要
2）臨床試験デザインの検討
少数例で有効性を検証する臨床試験方法の開発
3）サロゲートマーカーの開発
皮膚生検による末梢神経の形態およびmRNA発現による評価法の開発・改良
4）遺伝子治療を含む新規治療法の開発
・蛋白発現のコントロール：PMP22発現抑制物質のスクリーニング
・変異アレルの発現抑制：siRNA、deoxribozymes、Antisense oligonucleotides（ASO）、RNA trans-splicingアプローチなど
・欠損遺伝子・蛋白の補充：欠失している遺伝子の導入、既存薬の応用
・凝集体形成抑制：凝集体形成や蛋白折りたたみ異常機序の解明とその阻害物質の探索
5）リハビリテーションの有効性に関するエビデンスの蓄積
・病型別リハビリテーションプログラムの開発
・ロボット工学の活用：歩行サポートロボット装具などの改良・活用
6）外科治療、装具療法の開発・改良とエビデンスの蓄積
7）CMTに対する医療・福祉サービスの充実
8）CMTに関する啓発活動の充実

内反凹足に対して、足底解離術、筋腱移行術、骨切り術（中足骨骨切り術、踵骨骨切術）、三関節固定術（変形が高度で軟部組織手術や骨切術によって十分な矯正が得られない場合に適応）、創外固定術（イリザロフ法）などがある。鉤爪変形に対する手術には、長母趾伸筋腱を切離し、中足骨頭に作製した骨孔を通して固定する方法や長趾伸筋腱を切離し、第3楔状骨に固定する方法がある。鷲手（鉤爪手）変形に対して、腱移行術、関節固定術、軟部組織解離術が行われる。CMTでは、臼蓋形成不全を合併することがある。臼蓋形成不全に対して、骨盤骨切り術、大腿骨骨切り術が行われる。高度の脊柱側弯・後弯に対して脊椎固定術が行われることがある。

術後療法：筋腱移行術の場合は、約6週間のギプス固定後に歩行訓練、筋力訓練などのリハビリを行う。骨切り術・関節固定術の場合は5～6週間のギプス固定後に、歩行用ギプスを装着し歩行訓練を開始する。約10週後に骨癒合を確認しギプスを除去する。内反尖足の外科治療はCMT患者により安定した歩行をもたらすと考えられるが、その手術適応や外科的治療施行時期についてのより明確の基準作成が必要とされている[8]。

CMT患者が手術や出産などのために麻酔を受ける際にも注意が必要である。一般的に、脊髄くも膜下麻酔や硬膜外麻酔は避ける方がよいと言われている。全身麻酔時の入眠剤、静脈麻酔薬、筋弛緩薬に対する感受性が高いCMT患者がいる場合があるので注意が必要である。嚥下反射の減弱・声帯麻痺・胸鎖乳突筋の筋力低下、自律神経障害による不整脈・低血圧、側彎症による拘束性換気障害、悪性高熱症、術後呼吸不全などに注意が必要である。しかし、脊髄くも膜下麻酔、硬膜外麻酔、吸入麻酔のみ、全静脈麻酔＋神経ブロックなどで安全に手術が行われた例も報告されている。今後、CMTに対する適切な麻酔法に関する再検討・再評価が必要である。

CMTのリハビリテーション

CMTの筋力低下の特徴は、大腿部下1/3以下の筋萎縮・筋力低下、筋萎縮と筋力の不均衡により生じる凹足・内反、下垂足による鶏歩であり、それに廃用症候群が加わることが多い。CMTのリハビリテーションに関する研究はRCTレベルでは不十分であるが、週3回24週のリハビリテーションプログラムに参加することにより、膝関節伸展筋力の改善と大腿筋力の自覚症状の改善がみとめられたとの報告がある[9]。

CMTの筋力強化訓練は、低負荷・高頻度が基本である。軽度の障害の場合は、仕事や学業を積極的に行うことで筋力は維持されることが多い。一般的に、翌日に疲労を残さない程度の軽い運動療法は、筋力維持に役立つ可能性がある。可能な範囲は自分で歩くこと、自分のことは自分で行う、毎日一定時間散歩、固定自転車こぎなどの定期的な運動などがよいとされる。進行例では廃用症候群を避け筋萎縮・筋力低下を防止することが重要となる。廃用症候群の予防目的に、椅子からの立ち上がり訓練を行い臀筋・大腿四頭筋を強化する。手内筋の筋力低下に対しては、書字や箸の使用などの細かい動作の訓練や粘土細工などによる訓練が有効である。一方、CMT患者では筋力低下や心肺機能低下のため疲労を生じやすい。最大酸素摂取量の50%程度の運動負荷強度が最適な有酸素運動とされている。翌日に疲労が残らない程度の負荷強度で10～30分間行う。この際に個人の能力に合わせた時間の設定が重要である。過用性筋力低下にも注意が必要である。運動翌日に普段とは異なる筋力低下、筋肉痛、疲労感などを認める場合や血液中CK値が普段よりも急に高くなった場合には、運動や生活強度が過剰であると判断し運動量を減らす必要がある。

CMTの関節可動域制限の予防のために、発症早期から下腿三頭筋の持続伸張訓練を行う必要がある。また、踵の高い靴を履かないよ

うにすることも重要である。足関節の背屈方向へのストレッチ、手指MP関節屈曲方向へのストレッチ、母指の対立位保持、股関節の伸展方向へのストレッチ、膝関節の伸展方向へのストレッチなどが推奨される。関節可動域訓練に先行して温熱療法を行ことで組織の伸張性を増すことができる。ホットパック、極超短波、パラフィン浴を下腿や大腿の後部に15～20分間行う。関節可動域訓練、温熱療法などを十分量実施しても関節可動域の改善が難しければ、アキレス腱延長術などの外科的治療も検討する必要がある。

歩行時の転倒に対しては、装具療法、杖などの歩行補助具の適切な使用が転倒予防に有効である。CMTでは手内筋の萎縮があるので松葉杖やロフストランドクラッチ、プラットホーム型クラッチが推奨される。歩行器はキャスター付きの四輪型歩行器がよい。肢位の改善、関節の変形防止、疼痛改善などの目的で下肢装具が有効なことが多い。初期の段階では、ブーツやハイカット靴、足アーチサポートをつけた特注靴、中敷き（足底板）などで歩行の安定性が増加する。進行に応じて、足関節サポーター、短下肢装具、長下肢装具、ロフストランド杖の使用を検討する。ある程度長い距離を移動するには車椅子も考慮する方が関節の負担や筋疲労の軽減のためによい場合もある。骨折による廃用性障害が筋力低下を進めることになるので、転倒の注意と安定したフットウェアや装具を選ぶことが日常生活上重要である。

上肢装具では、屈筋群の緊張が高まり指の変形が進行することを予防し、残っている指運動の実用上の巧緻性を維持するために手関節装具を装着することが有効な場合がある。

CMTに対するロボット技術の応用

CMTには、「下肢自立支援ロボット」、「下肢訓練支援ロボット」の適応がある。下肢自立支援ロボットでは、入浴や移乗の支援をするロボット：レジーナ®（日本ロジックマシン）、ロボットスーツHAL®（筑波大学）：Hybrid Assistive Limb（HAL）がある。HAL®は、近位筋の障害もある重度障害のCMT患者に適応があることが報告された[10]。下肢訓練支援ロボットでは、TEM（安川電機）、リハボット（山梨大学）、Gait trainer（Free University）、Locomat（Hocoma）、歩行支援ロボット（安川電機・産業医科大学）などが開発されている。平成23年度に厚生労働省難治性疾患克服研究事業として、「神経・筋難病疾患の進行抑制治療効果を得るための新規医療機器、生体電位等で随意コントロールされた下肢装着型補助ロボットに関する治験準備研究」班（研究代表者　中島　孝先生）が組織され、補助ロボット技術の神経筋疾患への適応が検討されつつある。

CMT患者の日常生活の工夫、社会資源の利用

CMTに対する有効な薬物療法は未だ開発されていないが、少しでもよい健康状態を維持することは重要である。適切な運動負荷が症状を改善する可能性があり、日常的な運動の習慣を持つことは重要であると考える。食事療法では、CMT患者は消費カロリー／日が健常者より有意に少なく、メタボリック症候群が多い傾向がみられる。「現在の体重を維持する」ことが重要である。体重増加はすでに負担がかかっている足・膝関節や筋肉に対して、さらに負担をかけ、疼痛、疲労の増加に加えて、転倒や骨折のリスクを高める。CMTでは筋力低下から運動量が限られているため、一旦増加した体重を運動により減量することが極めて困難である。手足のケアでは、四肢遠位の冷感・浮腫、外傷、胼胝や潰瘍の形成に注意する。深部静脈血栓症とそれに関連する肺塞栓症にも注意が必要である。CMTでは、拘束性換気障害や中枢性睡眠時無呼吸症候群を来たし、パルスオキシメーター、非侵襲的換気療法が必要となる場合もある。

社会資源の有効な利用法の一例を以下に示す。身体障害者手帳の制度：携帯電話の基本使用料などの割引、鉄道やバス、飛行機の運賃割引など。障害者自立支援制度：介護給付、訓練等給付、補装具費や自立支援医療費支給、訪問サービス、通所サービスなど。身体障害者手帳、医師の意見書、106項目のアセスメント調査が必要である。医療費補助：CMTは特定疾患の指定を受けていない。例外として、東京都では「遺伝性ニューロパチー」として難病医療費助成の制度がある。身障手帳1・2級で「重度心身障害者」手続きを行うと医療費の助成が受けられる。福祉用具：治療用（訓練用）装具、更生用装具がある。T字杖は「日常生活用具」、多点杖・ロフストランド杖・松葉杖などは「補装具」に分類される。電動車椅子と手動車椅子はいずれも「補装具」である。自動車の改造費の一部に対して自治体の助成を受けられることがある

わが国におけるCMT患者会である「CMT友の会」は2008年6月に設立され、現在の会員数は約200名である。「CMT友の会」の主な目的は、「患者のQOL向上」、「医療の発展」、「社会認知の向上」であり、具体的には『交流』と『情報発信』を中心に活動している（http://www.j-cmt.org.jp）。医療・研究機関との相互協力にも積極的に取り組んでいる。英国のCMT患者会は25年前に7名の会員で設立され、現在、1500名以上の会員を有している。毎年、神経内科医、整形外科医、小児科医、リハビリテーション医、理学・作業療法士、装具士、心理士などによる講演を含む総会を行っている。米国のCMT患者会は、約15000名の会員を有し、英国のCMT患者会同様に活発な活動を行っている。

CMTと遺伝カウンセリング

CMT患者会の調査では、遺伝子検査を受けている患者はわずかに26.7%であった。遺伝に関する適切な理解が得られていない場合が多く、生涯独身を貫くなど結婚・出産に否定的に考える傾向がうかがえる。また、自分を産んだ親を受け入れられないなどの反応がみられる。CMTの早期診断、早期治療を考える場合、着床前診断、発症前診断などの遺伝子診断の倫理的問題は避けられず、遺伝カウンセリングの充実が必要である。

欧米に比べるとわが国では、CMTに対する医療従事者および一般社会の認知が十分ではないと思われる。最近、厚労省研究班から「シャルコー・マリー・トゥース病診療マニュアル」[1]が発刊されたが、今後、その普及が期待される。

CMTの治療とケアには、神経内科医、整形外科医、リハビリテーション医、そして基礎研究者の協力が必要であり、まさしく本学会の目指すものと一致している。本学会員がCMTの治療とケアに大いに貢献して頂くことを期待するものである。

文　献

1) シャルコー・マリー・トゥース病診療マニュアル．CMT診療マニュアル編集委員会編，2010，京都，金芳堂，京都，2010.
2) Saporta AS, Sottile SL, Miller LJ, Feely SM, Siskind CE, Shy ME. Charcot-Marie-Tooth disease subtypes and genetic testing strategies. *Ann Neurol* 2011; 69: 22-33.
3) Passage E, Norreel JC, Noack-Fraissignes P, *et al.* Ascorbic acid treatment corrects the phenotype of a mouse model of Charcot-Marie-Tooth disease. *Nat Med* 2044; 10: 396-401.
4) Sahenk Z, Nagaraja HN, McCracken BS, *et al.* NT-3 promotes nerve regeneration and sensory improvement in CMT1A mouse models and in patients. *Neurology* 2005; 65: 681-689.
5) Sereda MW, Meyer zu Hörste G, Suter U, *et al.* Therapeutic administration of progesterone antagonist in a model of Charcot-Marie-Tooth disease (CMT-1A). *Nat Med* 2003; 9: 1533-1537.

6) Khajavi M, Shiga K, Wiszniewski W, *et al*. Oran curcumin mitigates the clinical and neuropathologic phenotype of the Trembler-J mouse: a potential therapy for inherited neuropathy. *Am J Hum Genet* 2007; 81: 438-453.
7) Schenone A, Nobbio L, Monti Bragadin M, Ursino G, Grandis M. Inherited neuropathies. *Curr Treat Options Neurol* 2011; 13: 160-179.
8) 渡邉耕太，山下敏彦．シャルコー・マリー・トゥース病の外科的治療．*Peripheral Nerve* 2011; 22(1): 22-30.
9) Lindeman E, Leffers P, Spaans F, *et al*. Strength training in patients with Myotonic Dystrophy & Hereditary Motor & Sensory Neuropathy: A randomized clinical trial. *Arch Phys Med Rehabil* 1995; 76: 612-620.
10) 松嶋康之，蜂須賀研二．シャルコー・マリー・トゥース病のリハビリテーション．*Peripheral Nerve* 2011; 22: 31-38.

＜シンポジウム 17—2＞難治性末梢神経疾患の治療戦略

Charcot-Marie-Tooth 病の治療戦略

中川　正法

(臨床神経 2011;51:1015-1018)
Key words：CMT，遺伝子診断，治療，リハビリテーション，ブレインマシンインターファイエス

シャルコー・マリー・トゥース（Charcot-Marie-Tooth：CMT）病は，1886 年に Charcot，Marie，Tooth によって報告された世界中でみられる遺伝性ニューロパチーである．その有病率は 1/2,500 人ともいわれて，世界中に約 260 万人の CMT 患者がいると推定されている．CMT の原因遺伝子は 40 種類以上が特定され，わが国においても CMT の遺伝子診断に関しては大きな進展がみられている．しかし，CMT の遺伝子診断の情報や治療法の開発状況，外科療法やリハビリテーションなどに関する情報が医療関係者，CMT 患者に広く知られているとはいいがたく，単純に「CMT の治療法はない」と考えている医療関係者，CMT 患者が多いのではないかと思われる．今回のシンポジウムでは，CMT の遺伝子診断，内科的治療，外科的治療，リハビリテーションについて概説し，わが国と英国の CMT 患者会についても紹介する．

CMT の遺伝子診断

CMT は，電気生理学的検査所見に基づいて脱髄型，軸索型，中間型に大別される．脱髄型 CMT では，一般的に正中神経の運動神経伝導速度は 38m/s 以下，活動電位はほぼ正常または軽度低下を示し，腓腹神経所見では節性脱髄，onion bulb の形成をみとめる．軸索型 CMT では，同神経伝導速度は正常または軽度低下を示すが活動電位は明らかに低下し，腓腹神経所見では有髄線維の著明な減少を示す．しかし，いずれとも分けられない中間型 CMT も存在する（Fig. 1）．CMT のばあい，各病型である程度の臨床的特徴はあるものも臨床所見のみで確定診断をおこなうことが困難なことも多い[1]．末梢神経障害をしめす例では，家族歴の有無にかかわらず孤発例であっても，疾患の鑑別のために遺伝子学的検討をおこなう必要がある．鹿児島大学の高嶋らは遺伝性ニューロパチー遺伝子診断チップを開発し，全国的な遺伝性ニューロパチーデーターベースを構築しつつある．

内科的治療

もっとも頻度が高い CMT1A は *PMP22* の重複によってひきおこされる病態であり，アスコルビン酸が CMT1A モデルマウスに有効であると報告されて以降[2]，国内外で臨床試験がおこなわれた．わが国でも厚生労働省精神神経疾患研究委託費「難治性ニューロパチーの病態に基づく新規治療法の開発」研究班のもとで，「Charcot-Marie-Tooth 病 1A に対するアスコルビン酸の安全性・有効性に関する臨床試験」(UMIN 試験 ID：UMIN000001535)がおこなわれた．残念ながら，プライマリーエンドポイントである Charcot-Marie-Tooth Neuropathy Score (CMTNS)に有意な改善はなくアスコルビン酸の有効性は確認できなかった．海外でのアスコルビン酸投与試験でもアスコルビン酸の有効性は証明されなかった．アスコルビン酸が CMT1A に無効なのか，アスコルビン酸の投与期間・量の問題なのかに関する検討が今後必要である．わが国でおこなった臨床試験では，右握力は有意に改善しており，ある程度の効果はあるのではないかと考えられる．現在，軸索興奮性を測定する Qtrac プログラム（ミユキ技研）をもちいて非利き手正中神経において運動神経の軸索興奮性測定し，アスコルビン酸（20mg/kg/日）投与前後での変化を検討中である．

その他，Neurotrophin-3(NT-3)[3]，プロゲステロン拮抗薬[4]，クルクミン[5]などが CMT に試みられている．

患者数が少ない CMT のばあい，臨床試験デザインについても検討する必要がある．最近の RCT では，皮膚生検による末梢神経の形態および mRNA 発現の評価がおこなわれているが，今後，新しいサロゲートマーカーの開発も必要である．

遺伝子治療をふくむ新規治療法として，各病型の分子病態の解明に基づいて，1)蛋白発現のコントロール：*PMP22* 発現抑制物質のスクリーニングなど，2)変異アレルの発現抑制：siRNA，deoxribozymes，Antisense oligonucleotides(ASO)，RNA trans-splicing アプローチなど，3) 欠損遺伝子・蛋白の補充：欠失している遺伝子の導入，既存薬の応用，4)凝集体形成抑制：凝集体形成や蛋白折りたたみ異常の阻害物質の探索などが期待される[6](Table 1)．

外科的治療，リハビリテーションなど

関節変形が進行し，装具をもちいても足を適切な位置に保てず歩行に支障が出てきたばあい，関節の安定性を図るために腱延長術や骨切り術などの整形外科手術が適応となるばあいがある．外科治療が一般的に長期的な効果を有するかどう

京都府立医科大学大学院神経内科学〔〒602-0841　京都市上京区河原町通広小路上ル梶井町 465〕
（受付日：2011 年 5 月 19 日）

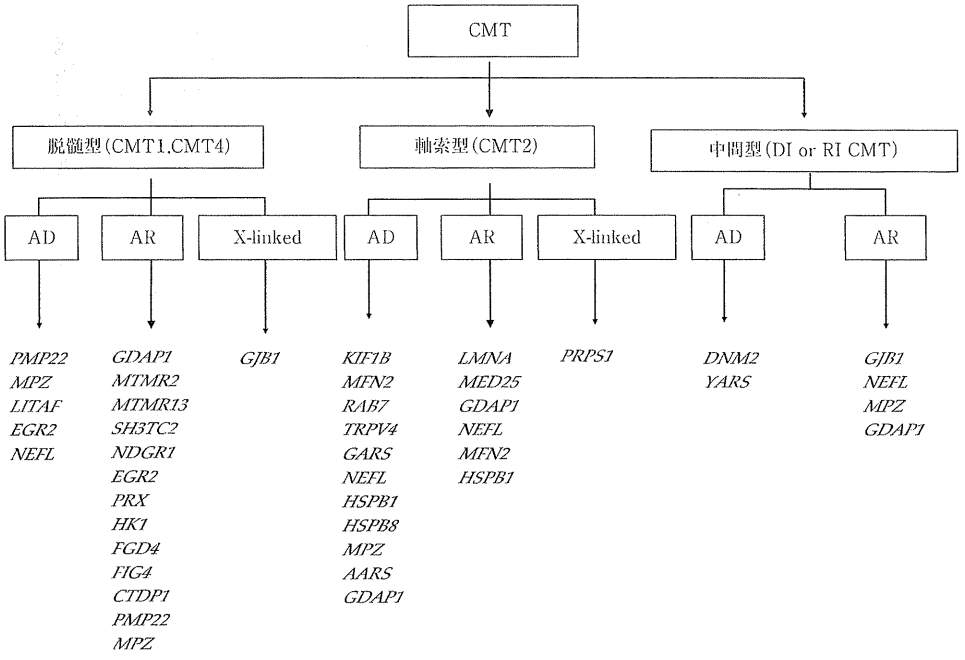

Fig. 1　CMT の病型と遺伝子異常．同じ遺伝子でもことなる病型または遺伝子型をとることがある．
J Peripheral Nervous System 16：1-14，2011 より引用改変

Table 1　Charcot-Marie-Tooth 病（CMT）の治療戦略．

CMT の遺伝子診断を踏まえて以下のような事項が CMT の治療戦略として必要である．

1）CMT の病型別自然経過の解明
　疾患頻度が低い CMT 病型も多く，その自然経過を明らかにするためには国際共同研究が必要
2）臨床試験デザインの検討
　少数例で有効性を検証する臨床試験方法の開発
3）サロゲートマーカーの開発
　皮膚生検による末梢神経の形態および mRNA 発現による評価法の開発・改良
4）遺伝子治療をふくむ新規治療法の開発
　・蛋白発現のコントロール：*PMP22* 発現抑制物質のスクリーニング
　・変異アレルの発現抑制：siRNA，deoxribozymes，Antisense oligonucleotides（ASO），RNA trans-splicing アプローチなど
　・欠損遺伝子・蛋白の補充：欠失している遺伝子の導入，既存薬の応用
　・凝集体形成抑制：凝集体形成や蛋白折りたたみ異常機序の解明とその阻害物質の探索
5）リハビリテーションの有効性に関するエビデンスの蓄積
　・病型別リハビリテーションプログラムの開発
　・ロボット工学の活用
　　歩行サポートロボット装具などの改良・活用
6）外科治療，装具療法の開発・改良とエビデンスの蓄積
7）CMT に関する啓発活動の充実

かについては現時点では十分なエビデンスはない．外科手術の長所と短所を CMT 患者，家族と十分に検討した上で施行することが重要である．

肢位の改善，関節の変形防止，疼痛改善などの目的で下肢装具が有効なことが多い．初期の段階では，ブーツやハイカット靴，足アーチサポートをつけた特注靴，中敷き（足底板）などで歩行の安定性が増加する．進行に応じて，足関節サポーター，短下肢装具，長下肢装具，ロフストランド杖の使用を検討する．ある程度長い距離を移動するには車椅子も考慮する方が関節の負担や筋疲労の軽減のためによいばあいもある．骨折による廃用性障害が筋力低下を進めることになるので，転倒への注意と安定したフットウェアや装具を選ぶことが日常生活上重要である．

上肢装具では，屈筋群の緊張が高まり指の変形が進行することを予防し，残っている指運動の実用上の巧緻性を維持するために手関節装具を装着することが有効なばあいがある．

CMT のリハビリテーションに関する研究は RCT レベルでは不十分である．一般的に，翌日に疲労を残さない程度の軽い運動療法は，筋力維持に役立つ可能性がある．週 3 回 24 週のリハビリテーションプログラムに参加することにより，膝関節伸展筋力の改善と大腿筋力の自覚症状の改善がみとめられたとの報告がある．最近，ロボットスーツ「HAL®」の利用が可能になったが，CMT 患者への応用に関する研究班が組織され検討が開始された．

CMT 患者会活動

わが国における CMT 患者会である「CMT 友の会」は 2008 年 6 月に設立され，現在の会員数は約 200 名である．「CMT 友の会」の主な目的は，「患者の QOL 向上」，「医療の発展」，「社会認知の向上」であり，具体的には『交流』と『情報発信』を中心に活動している（http://www.j-cmt.org.jp）．医療・研究機関との相互協力にも積極的に取り組んでいる．英国の CMT 患者会は 25 年前に 7 名の会員で設立され，現在，1,500 名以上の会員を有している．毎年，神経内科医，整形外科医，小児科医，リハビリテーション医，理学・作業療法士，装具士，心理士などによる講演をふくむ総会をおこなっている．

その他の問題点

CMT 患者が他の内科疾患などに罹患したばあいに使用される薬剤が末梢神経障害を悪化させるばあいがある．とくにビンクリスチンなどが CMT の症状を悪化させる薬剤として有名である（http://www.charcot-marie-tooth.org/med_alert.php）．最近，抗癌薬の投与により末梢神経障害が顕在化し，CMT の遺伝子変異が明らかとなった例が報告されている．

CMT の早期診断，早期治療を考えるばあい，着床前診断，発症前診断などの遺伝子診断の倫理的問題は避けられず，遺伝カウンセリングの充実も必要である．欧米にくらべるとわが国では，CMT に対する医療従事者および一般社会の認知が十分ではないと考えられるが，最近，「シャルコー・マリー・トゥース病診療マニュアル」[7]が発刊され，その普及が期待される．

文　献

1) Saporta AS, Sottile SL, Miller LJ, et al. Charcot-Marie-Tooth disease subtypes and genetic testing strategies. Ann Neurol 2011;69:22-33.
2) Passage E, Norreel JC, Noack-Fraissignes P, et al. Ascorbic acid treatment corrects the phenotype of a mouse model of Charcot-Marie-Tooth disease. Nat Med 2004;10:396-401.
3) Sahenk Z, Nagaraja HN, McCracken BS, et al. NT-3 promotes nerve regeneration and sensory improvement in CMT1A mouse models and in patients. Neurology 2005;65:681-689.
4) Sereda MW, Meyer zu Hörste G, Suter U, et al. Therapeutic administration of progesterone antagonist in a model of Charcot-Marie-Tooth disease (CMT-1A). Nat Med 2003;9:1533-1537.
5) Khajavi M, Shiga K, Wiszniewski W, et al. Oran curcumin mitigates the clinical and neuropathologic phenotype of the Trembler-J mouse: a potential therapy for inherited neuropathy. Am J Hum Genet 2007;81:438-453.
6) Schenone A, Nobbio L, Monti Bragadin M, et al. Inherited neuropathies. Curr Treat Options Neurol 2011;13:160-179.
7) CMT 診療マニュアル編集委員会，編．シャルコー・マリー・トゥース病診療マニュアル．京都：金芳堂；2010.

Abstract

Therapeutic strategies for Charcot-Marie-Tooth disease

Masanori Nakagawa, M.D.
Department of Neurology, Graduate School of Medical Science, Kyoto Prefectural University of Medicine

Recently, causative gene discovery and genetic diagnosis system for Charcot-Marie-Tooth disease (CMT) have been rapidly developed. These genetic information and research progress, however, have not been informed to medical staff and CMT patients. CMT-Japan, which is an association of Japanese CMT patients, has been organized in 2008. Many of CMTJ members have not been diagnosed genetically. Most of medical staff and CMT patients may imagine that there is no hope for the CMT feature. Research on CMT therapy, however, has been progressing such as clinical trial of ascorbic acid, and experimental trial of curcumin and antiprogesterone. The development of robot technology and brain machine interface open a new way of therapy for CMT. Elucidation of molecular mechanisms and finding of effective treatments for CMT using cell culture, iPS cell, animal model, agents to suppress *PMP22* expression, and read-through of stop codon methods are expected in the near features. In addition, development of surrogate markers, improvement of clinical trial design, establishment of nationwide diagnostic system, and assessment of natural history with international collaboration study must be done as soon as possible. CMT management manual, review of CMT research, open seminar for CMT, and genetic counseling are essential to improve the medical management for CMT. The collaboration among medical engineers, neurophysiologists, rehabilitation team, orthopedist, neurologists, genetic researchers and CMT patients and their families is of cardinal importance to achieve these studies for CMT.

(Clin Neurol 2011;51:1015-1018)

Key words: CMT, genetic diagnosis, therapy, rehabilitation, brain machine interface

Biochemical and Biophysical Research Communications 405 (2011) 697–702

Contents lists available at ScienceDirect

Biochemical and Biophysical Research Communications

journal homepage: www.elsevier.com/locate/ybbrc

Axotomy induces axonogenesis in hippocampal neurons by a mechanism dependent on importin β

Ryo Ohara [a,b], Katsuhiko Hata [a], Noriko Yasuhara [c,d], Rashid Mehmood [c,d], Yoshihiro Yoneda [c,d], Masanori Nakagawa [b], Toshihide Yamashita [a,e,*]

[a] Department of Molecular Neuroscience, Graduate School of Medicine, Osaka University, 2-2, Yamadaoka, Suita, Osaka 565-0871, Japan
[b] Department of Neurology, Graduate School of Medical Science, Kyoto Prefectural University of Medicine, Kyoto 602-0841, Japan
[c] Department of Frontier Bioscience, Graduate School of Frontier Bioscience, Osaka University, 1-3, Yamadaoka, Suita, Osaka 565-0871, Japan
[d] Department of Biochemistry, Graduate School of Medicine, Osaka University, 1-3, Yamadaoka, Suita, Osaka 565-0871, Japan
[e] JST, CREST, 5, Sanbancho, Chiyoda-ku, Tokyo 102-0075, Japan

ARTICLE INFO

Article history:
Received 22 January 2011
Available online 1 February 2011

Keywords:
Axonal injury
Axonogenesis
Dynein
Importin

ABSTRACT

We characterize the previously unrecognized phenomenon of axotomy-induced axonogenesis in rat embryonic hippocampal neurons in vitro and elucidate the underlying mechanism. New neurites arose from cell bodies after axotomy and grew. These neurites were Tau-1-positive, and the injured axons showed negative immunoreactivity for Tau-1. Axonogenesis was delayed in these neurons by inhibiting the dynein–dynactin complex through the overexpression of p50. Importin β, which was locally translated after axotomy, was associated with the dynein-importin α complex and was required for axonogenesis. Taken together, these results suggest that retrograde transport of injury-induced signals in injured axons play key roles in the axotomy-induced axonogenesis of hippocampal neurons.

1. Introduction

Restoration of neuronal polarization after disruption can be achieved through transformation of a dendrite into a new axon or by axonal regrowth following severance of an axon [1,2]. The cell body of an injured neuron must receive accurate and timely information about axonal damage in order to reproduce the polarization. A number of injury signals have thus far been postulated to underlie this process in injured peripheral neurons, including injury-induced discharge of axonal potentials, interruption of the normal supply of retrograde-transported target-derived factors (called negative injury signals), and retrograde injury signals traveling from the injury site back to the cell body (called positive injury signals) [3]. Interestingly, injury to neurons located in the peripheral branch of the dorsal root ganglion (DRG) followed by injury to the central branch leads to promotion of central axon regeneration [4,5]. This phenomenon, called the "conditioning lesion paradigm," suggests that injury signals transported from the injury site back to the cell body increase the intrinsic growth capacity of the neurons. Further, microinjection of lesion-induced axoplasmic proteins elicits growth and survival responses in neural cell bodies [6], and retrogade axonal transport of a nuclear localization signal (NLS) protein has been reported in mammals [7]. Nuclear import of the protein is mediated by NLS binding to importins/karyopherins. Importin α binds the NLS within the cargo protein directly, and its affinity to NLS is increased through interaction with importin β, which facilitates transport of the complex through the nuclear pore complex [8,9]. Hanz et al. provided evidence that importins play key roles in the transport of some retrograde injury signals in rodent sciatic nerve [10]. Several importin α members exist in sensory axons in both control and injured sciatic nerves, in constitutive association with dynein motor proteins, whereas importin β1 protein is not detectable in control sciatic nerve axoplasm. Importin α protein is constitutively complexed with the retrograde motor dynein; upon lesion, importin β1 mRNA localized in the axoplasm is rapidly translated into importin β1 protein, leading to the formation of importin α/β1 heterodimers bound to the retrograde motor dynein. Thus, the axoplasmic importin–dynein complex enables retrograde injury signaling in injured sciatic nerve.

It has been widely recognized that a dendrite is transformed into a new axon or that an injured axon regrows after axonal injury [1,2]. In addition to these responses, we report here that new neurites arise from cell bodies after axotomy and become axons in cultured embryonic hippocampal neurons. Dotti et al. previously mentioned axonogenesis after axotomy but did not investigate further in their report [1]. Until now, little has been written about this phenomenon. Since cell bodies of injured neurons must receive the signals for axonal damage in order to produce new axons, we believe that an injury signal may be transported retrogradely back

* Corresponding author at: Department of Molecular Neuroscience, Graduate School of Medicine, Osaka University, 2-2, Yamadaoka, Suita, Osaka 565-0871, Japan. Fax: 81 6 68793669.
E-mail address: yamashita@molneu.med.osaka-u.ac.jp (T. Yamashita).

0006-291X/$ - see front matter © 2011 Elsevier Inc. All rights reserved.
doi:10.1016/j.bbrc.2011.01.108

to the cell body by the dynein–dynactin complex. In the present study, we characterize this axotomy-induced axonogenesis and elucidate the underlying mechanism.

2. Materials and methods

2.1. Plasmid constructs

The cDNAs encoding rat dynamitin (p50) were amplified by PCR from a rat brain cDNA library. The amplified cDNAs were subcloned into pAcGFP1-N1 (Clontech) and were named pAcGFP-dynamitin (p50)-N1. pGFP-Bimax2-C2, a plasmid expressing Bimax2 (peptide inhibitor of importin) conjugated to GFP, was made according to a previous report [15].

2.2. Dissociated cell culture

All the experimental procedures were approved by the Institutional Ethics Committee of Osaka University. Hippocampal neurons obtained from Wistar rat pups on E18–19 were dissociated by trypsinization (treatment with 0.25% trypsin in PBS for 15 min at 37 °C) followed by resuspension in DMEM/F12 (Invitrogen) containing 10% FBS, and trituration. Subsequently, the neurons were washed three times. The cells were suspended in DMEM/F12 containing 10% FBS, plated on poly-L-lysine and laminin-coated dishes, and maintained at 37 °C in 5% CO_2. The culture medium was replaced with a serum-free DMEM/F12 supplemented with B27 (Invitrogen) 12 h after plating, when the cells had attached. Cells were pretreated with each 1 μg/ml CHX (Nakarai Tesque) or 0.1 μg/ml AMD (Nakarai Tesque) for 30 min before axotomy.

2.3. Explant culture

The hippocampus was removed from Wistar rat pups on E18 according to a previously reported method with a slight modification [11]. The hippocampus was chopped into 300–600 μm-sized pieces using fine tweezers. These pieces were then placed in a 3.5 cm tissue culture dish containing 1.5 ml of DMEM/F12 supplemented with 10% FBS. After two days of incubation at 37 °C in a 5% CO_2 incubator, the medium was replaced with DMEM/F12 supplemented with 2% B27. At 10 DIV, the extended neurites were transected using a blade according to a previously reported method [12].

2.4. Nucleofection procedure

For each transfection experiment, 4.0–5.0 × 10^6 cells were used with the Nucleofector II™ (Amaxa Biosystems). Dissociated hippocampal neurons were spun down at 800 rpm for 3 min, and the medium was removed. Cells were then resuspended in 100 μl of rat neuron Nucleofector™ solution (Amaxa Biosystems) at RT, followed by addition of 5 μg of pAcGFP-dynamitin (p50)-N1 or pGFP-Bimax2-C2. The mixture of hippocampal neurons, Nucleofector™ solution, and the plasmids was transferred to a 2-mm electroporation cuvette (Amaxa Biosystems), inserted in the Nucleofector,™ and processed with program O-03. Immediately after transfection, 1 ml of DMEM/F12 supplemented with 10% FBS was added to the hippocampal neurons to reduce damage, and the cells were plated on poly-L-lysine and laminin-coated dishes. The culture medium was replaced with serum-free DMEM/F12 supplemented with B27 3 h after plating to reduce damage to the cells.

2.5. Axotomy and time-lapse imaging

The culture dish was secured in a chamber that was supplied continuously with 5% CO_2 in air. The chamber was placed on an Olympus IX81 inverted phase-contrast microscope equipped with a heated stage apparatus (model MI-IBC-IF, Olympus). We chose 10–15 polarized hippocampal neurons in each dish at three DIV and cut the axons of the neurons by using a 30 G needle through the microscope. Images of the axotomized neurons were acquired every 3 min for 12 h using a 40× objective lens with a charge-coupled device video camera (Cooke). Images were combined into a time-lapsed sequence using MetaMorph software (Molecular Devices).

2.6. Fluorescence immunostaining

Cells were fixed in 2% paraformaldehyde and 2% sucrose in 0.1 mol phosphate buffer for 20 min at RT and incubated with a blocking solution containing 5% BSA and 0.1% Triton-X in PBS for 1 h, followed by overnight incubation at 4 °C with anti-importin α4 antibody (diluted 1:1000 in the blocking solution; Everest Biotech), anti-importin β1 antibody (diluted 1:1000 in the blocking solution; Thermo Scientific) and anti-Tau1 antibody (diluted 1:1000 in the blocking solution; Chemicon International). Following primary antibody incubation, sections were washed three times with PBS, and fluorescent dye Alexa 488-conjugated anti-rabbit IgG (diluted 1:1000 in 5% bovine serum albumin in PBS; Molecular Probes/Invitrogen) at room temperature for 1 h. They were then observed with an Olympus IX81 inverted phase-contrast microscope.

2.7. Western blotting

Cells were lysed with 50 mmol Tris–HCl (pH 7.4), 150 mM NaCl, 1% Np-40, 0.1% SDS, 2 mmol EDTA, 1 mmol Na3VO4, 1 mmol NaF, and a protease inhibitor mixture (Roche Diagnostics). The homogenate was centrifuged at 15,000 rpm for 10 min, and the supernatant was stored at −20 °C. The protein concentration was measured using a bicinchoninic acid protein assay kit (Pierce). Equal amounts of protein were loaded into each lane, run on SDS–PAGE, and then transferred to a polyvinylidene difluoride membrane (PVDF; Millipore). The protein samples were boiled in sample buffer for 5 min, run on SDS–PAGE, and then transferred to PVDF membranes (Millipore). The membranes were blocked for 1 h at RT with 0.5% skim milk, incubated for 2 h at RT with anti-importin β antibody (diluted 1:5000; Thermo Scientific), anti-dynein 74 kDa intermediate chains (1:1000; Millipore) and anti-α tubulin (diluted 1:1000; Santa Cruz Biotechnology). HRP-conjugated secondary antibodies (diluted 1:1000; Cell Signaling Technology) and ECL Plus reagents (GE Healthcare UK Ltd.) were used for detection. The membrane was exposed to X-ray film or the LAS-3000 image system according to the manufacture's specifications (Fujifilm).

2.8. Coimmunoprecipitation assay

Rat hippocampal explants were lysed in 50 mol Tris–HCl (pH 7.5), 150 mmol NaCl, 10% glycerol, and 1% NP-40 supplemented with protease inhibitor cocktail tablets (Roche Diagnostics). The lysates were incubated on a rocking platform at 4 °C for 20 min and clarified by centrifugation at 13,000×g at 4 °C for 10 min. The supernatants collected were precleared for 30 min by incubating with 60 μl of protein-G Sepharose beads (GE Healthcare UK Ltd.). After a brief centrifugation to remove the precleared beads, the cell lysates were incubated overnight (for coimmunoprecipitation with rat hippocampal explants extracts) at 4 °C with anti-dynein 74 kDa intermediate chain antibody (Millipore). The immunocomplexes were collected for 1 h at 4 °C with protein-G Sepharose beads that had been coated with 0.1% BSA in PBS. The beads were washed four times with lysis buffer. The bound proteins were solubilized with 1× sample buffer and subjected to SDS–PAGE followed by immunoblotting.

2.9. Morphometrical analysis

We classified the morphological changes of axotomized neurons into five groups as follows: axonogenesis, new neurites arose from cell bodies after axotomy and grew; dendrites change into axons, dendrites grew and became axons instead of axotomized axons; regrowth, axotomized axons regrew; no change, axotomized axons retracted or showed no morphological change; death, neurons died within 3 h after axotomy.

2.10. Statistical analysis

Significant differences in the data for axonogenesis after axotomy (Figs. 1C, 3A and J) were determined by χ^2 test. Significant differences in the other data were determined by Student's *t*-test (Figs. 2C, 3F and G).

3. Results

3.1. Axotomy induces axonogenesis in cultured hippocampal neurons

We cultured hippocampal rat neurons (embryonic day [E] 18–19) at low density for three days and cut the axons of the stage three polarized neurons. We then observed morphological changes in these neurons for 12 h using time-lapse imaging. Among 65 axotomized neurons excluding 10 neurons died within 3 h after axotomy, axotomized axons regrew in 35 neurons; the remaining dendrites became new axons in seven neurons; and new neurites arose from cell bodies after axotomy and grew (neuritogenesis) in eight neurons (Fig. 1A and B). This neuritogenesis was specific to axotomized neurons since it was never observed in 62 nonaxotomized neurons at the same stage (Fig. 1C). Immunocytochemistry for Tau-1 revealed that these new neurites had become axons (Fig. 1D); interestingly, the injured axons showed negative immunoreactivity for Tau-1. In the present manuscript, we term this phenomenon, which is characterized by axonogenesis in stage three hippocampal neurons after axotomy, axotomy-induced axonogenesis.

3.2. Dynein–dynactin complex is required for axotomy-induced axonogenesis

In our research, we aimed to explore the mechanism of axotomy-induced axonogenesis. As new neurites were induced from the cell body after axonal injury, we assumed that some sort of injury-induced signal was transported retrogradely via proximal axons to the cell bodies. If this was indeed the case, the dynein–dynactin complex, which is mainly involved in retrograde axonal transport, might contribute to transporting the signal. To assess this hypothesis, we overexpressed p50, which is one of the 11 subunits of the dynein–dynactin complex. Although its overexpression typically disrupts the dynein–dynactin complex [13], when p50

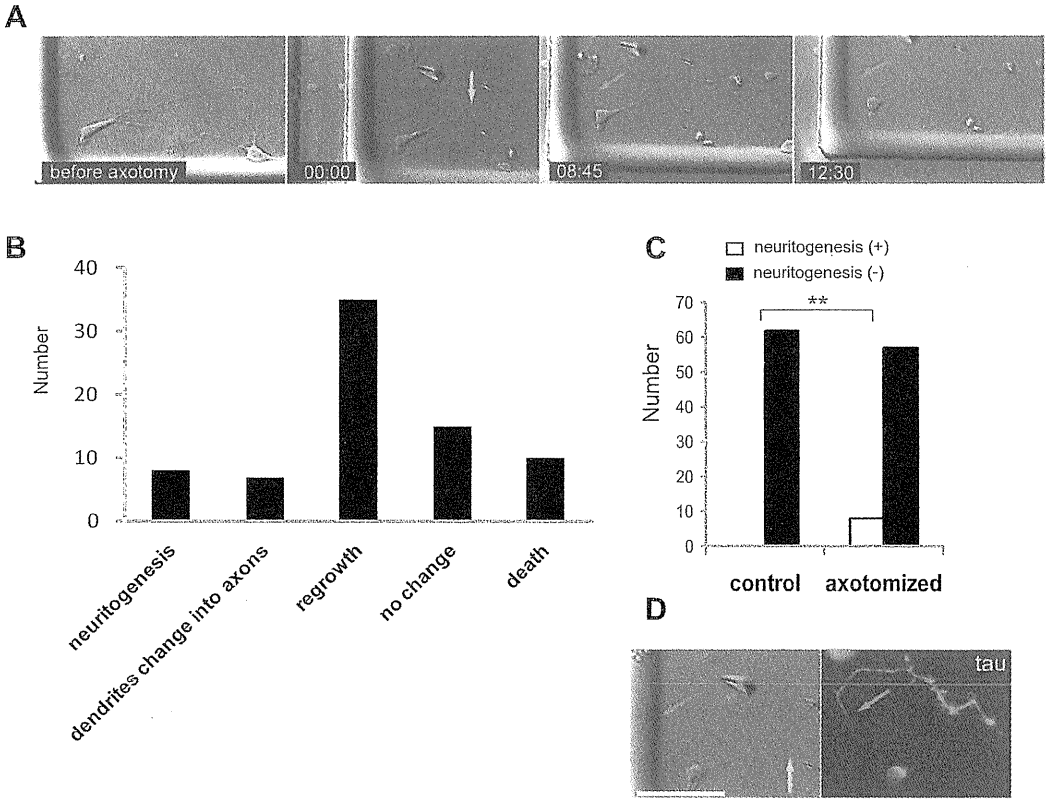

Fig. 1. Axonogenesis is induced by axotomy of cultured hippocampal neurons. (A) Time-lapse analysis of the neuritogenesis after axotomy. The hippocampal neurons were cultured for three days in vitro, followed by axotomy. A new neurite (pink arrow) arose from the cell body of the axotomized neuron and grew. The yellow arrow indicates the axotomized site. The time after axotomy is shown. Scale bar, 50 μm. (B) Various responses of axotomized neurons ($n = 75$). The graph shows the number of the neurons with the indicated morphological changes. Some transected axons regrew (regrowth), whereas some did not show any remarkable change (no change). Some neurons died within 3 h after axotomy. In some cases, a dendrite was transformed into a new axon, or a new axon arose from the cell body after axotomy and grew (neuritogenesis). (C) Neuritogenesis after axotomy occurred in eight neurons out of 65 axotomized neurons (10 dead neurons were excluded). Neuritogenesis never occurred in 62 nonaxotomized neurons. $^*p < 0.01$; χ^2 test. (D) The neuron in (A) was immunostained for Tau-1 13 h after the axotomy. The new neurite (pink arrow in A) became positive for Tau-1, and the injured neurite was negative for Tau-1. The yellow arrow indicates the axotomized site. Scale bar, 50 μm. (For interpretation of the references in color in this figure legend, the reader is referred to the web version of this article.)

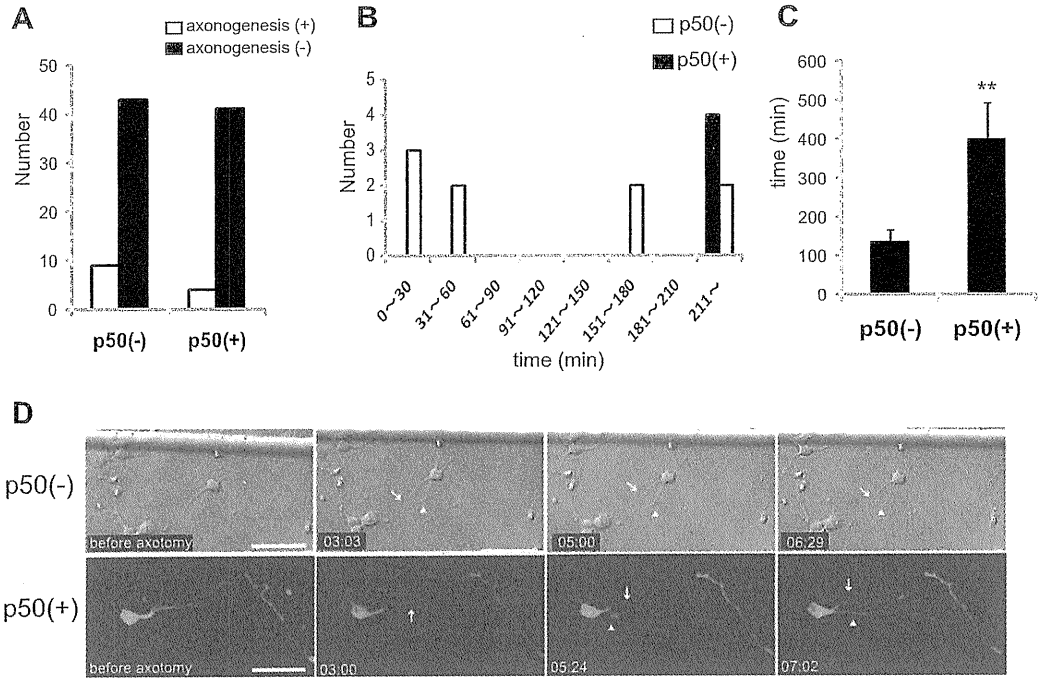

Fig. 2. Axotomy-induced axonogenesis is delayed by overexpression of p50. (A) The graph shows the number of neurons with or without axonogenesis after transfection with or without p50. The morphology of the neurons was estimated 12 h after axotomy. The difference in the number of neurons with axonogenesis between the two groups was not significant. (B) The graph shows the number of the neurons that induced new neurites at the indicated times. New neurites arose within 3 h after axotomy in seven out of nine neurons without p50 transfection (control). When p50 was overexpressed, new neurites arose after 4 h following axotomy in all four neurons. (C) The average time it took for a new neurite to arise after axotomy; $n = 4$, p50 (+); $n = 7$, p50 (−). Data are represented as mean ± SEM. $^{**}p < 0.01$, Student's t-test. (D) Time-lapse images of axotomized neurons. The arrows indicate the axotomized site, and arrowheads indicate the new neurites. Whereas new neurites had arose 3 h after axotomy in the control neurons (upper figures), new neurites began to arise at 5 h after axotomy in the p50-overexpressed neurons (lower figures). Scale bars, 50 μm.

was overexpressed in the neurons, the frequency of axotomy-induced axonogenesis was not statistically different from that of the control transected neurons without p50 overexpression (Fig. 2A). On the other hand, time-lapse analysis demonstrated that axonogenesis occurred within 3 h after axotomy in most of the neurons without overexpression of p50 while all the new axons arose more than 4 h after axotomy in the neurons transfected with p50 (Fig. 2B, D). The average time for axonogenesis after axotomy in p50-overexpressed neurons (400.75 ± 93.04 min) showed a significant delay compared with that of control transected neurons (136.42 ± 32.74 min) (Fig. 2C and D). These results suggest that overexpression of p50 suppressed retrograde transport by the dynein–dynactin complex, thereby inhibiting axonogenesis.

3.3. Importin β, which is locally translated after axotomy, associates with dynein

The above results support the notion that an injury-induced signal may be retrogradely transported to the cell body to induce axonogenesis. To further explore the molecular mechanism of this phenomenon, we assessed whether axotomy-induced axonogenesis required de novo protein synthesis or transcription. We employed actinomycin D (AMD) to inhibit transcription and used cycloheximide (CHX) to inhibit protein biosynthesis. Both inhibitors completely blocked injury-induced axonogenesis (Fig. 3A). These results suggest that axotomy-induced axonogenesis requires both the transcription and biosynthesis of protein. Injury-induced signals may therefore be transported via axons retrograde to the nucleus, leading to de novo protein synthesis in support of axonogenesis.

We were interested in what was transported from the injured axons to the cell body. Since it was previously reported that upon lesion of the sciatic nerve, importin β1 mRNA in axons is locally translated [10], we addressed whether this was the case in the axotomized hippocampal neurons. The neurons were immunostained for importin α4 and β1 (hereafter referred to as importin α and importin β). Expression of importin α was observed in the cell bodies as well as in the processes of nonaxotomized neurons at three days in vitro (DIV). On the other hand, importin β protein was observed in the cell bodies of nonaxotomized neurons, but not in the processes (Fig. 3B). In contrast, at 1 h after axotomy, some of the neurons expressed importin β in the axons just proximal to the injury site as well as in their cell bodies (Fig. 3C). This observation suggests that local protein synthesis of importin β occurs after axotomy of the hippocampal neurons.

Next, we evaluated the amount of importin β in the axotomized neurons. To obtain enough protein for western blotting, we employed an explant culture of the hippocampus from E18 rats. We cut the axons of the hippocampal explants with a blade (Fig. 3D) and separately collected the cell bodies, including the proximal axons, and the distal axons (refer to the schema in Fig. 3E) at 0 min, 5 min, 10 min, and 1 h after axotomy. The level of importin β was increased after axotomy in both the cell bodies and the distal axons (Fig. 3E–G). The level of importin β in the cell bodies, including the proximal axons, increased continuously during the observation period (~1 h) and that in the distal axons increased transiently (at 5 min), returning to the baseline level thereafter. As importin β was also increased in the distal axons, which were separated from the cell bodies, it was suggested that local protein synthesis occurred in the injured axons. The increase in the level of importin β 1 h after axotomy was completely inhibited by CHX but not AMD (Fig. 3H), further supporting the idea that importin β mRNA is translated in response to axotomy.

As importin α was diffusely expressed in the neurons, de novo synthesis of importin β may allow formation of importin α/β het-

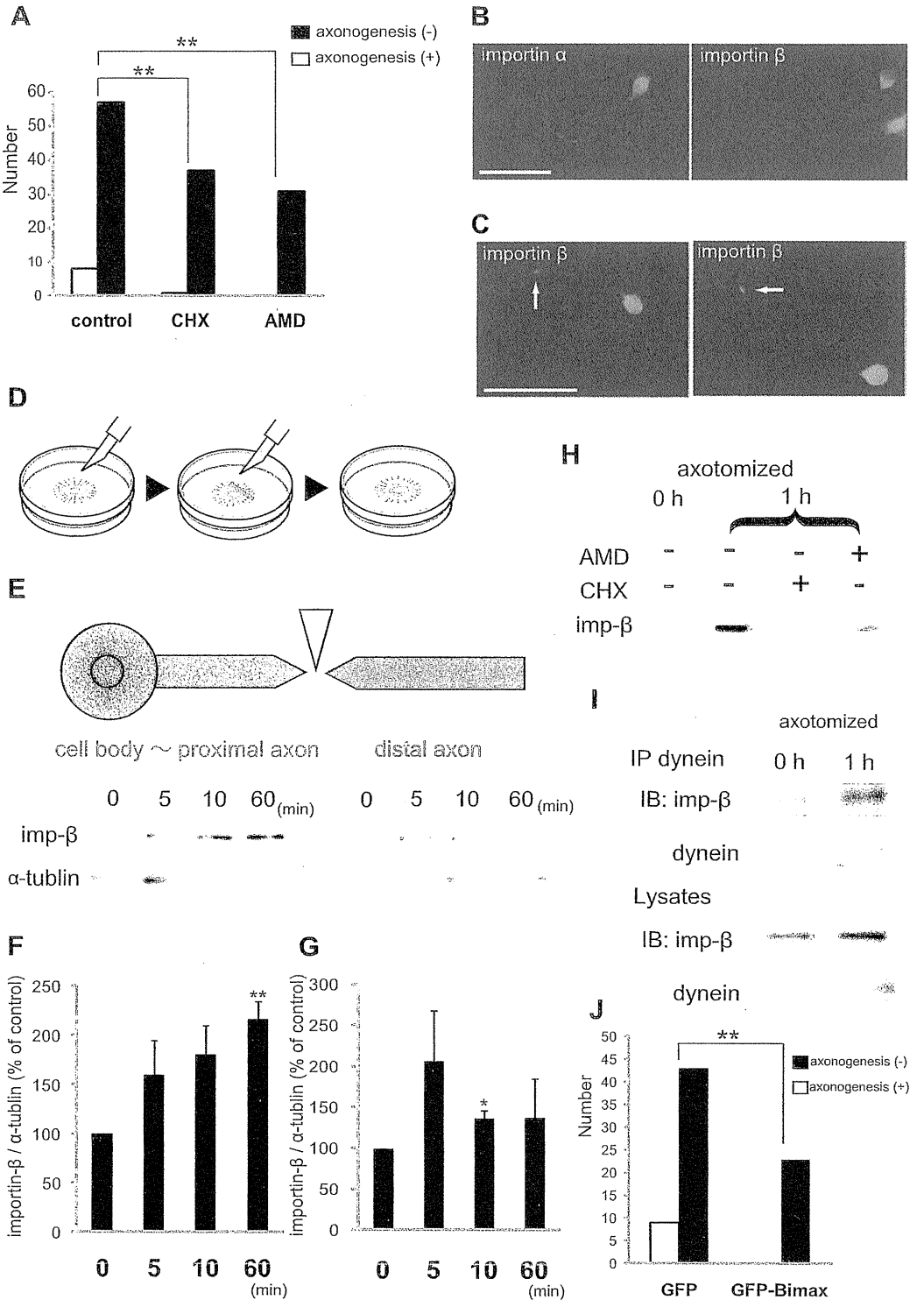

Fig. 3. Importin β is increased and associates with dynein. (A) The axonogenesis was attenuated by cycloheximide (CHX) or actinomycin D (AMD). The graph shows the number of neurons with or without axonogenesis. Twelve hours after adding 1 μg/ml CHX ($n = 38$) or 0.1 μg/ml AMD ($n = 31$) to the culture, axonogenesis was estimated. Control neurons ($n = 65$). $^{**}p < 0.01$; χ^2 test. (B) Immunostaining of a hippocampal neuron at three days in vitro reveals expression of importin α4 in the cell body and axon. Importin β was clearly found in the cell body, but not in the axon. Scale bar, 50 μm. (C) Immunostaining of neurons 1 h after axotomy revealed that importin β was increased at the tip of the injured axons (arrows). Scale bar, 50 μm. (D) Procedure for transfection of neurites from the explant. (E) Western blot analysis of lysates from axotomized hippocampal explants from 0 min to 1 h after axotomy. Lysates were obtained from cell bodies that included proximal as well as from distal axons. (F, G) The relative level of importin β in the cell bodies, including proximal axons (F) and distal axons (G). Data are represented as the mean ± SE of three independent experiments. $^{**}p < 0.01$; $^{*}p < 0.05$ compared with the control (Student's t-test). (H) Hippocampal explants were exposed to CHX or AMD for 30 min before axotomy and subjected to western blot 1 h after axotomy for the detection of importin β. (I) Coimmunoprecipitation of dynein with importin β. Lysates were prepared from hippocampal explants 1 h after axotomy. (J) The axonogenesis was inhibited by over-expression of Bimax. The graph shows the number of neurons with or without axonogenesis. Axonogenesis was estimated 48 h after nucleofection of GFP-Bimax. Neurons expressing GFP alone ($n = 52$), and neurons over-expressing Bimax ($n = 23$). $^{**}p < 0.01$; χ^2 test.

erodimers, which are associated with retrograde motor dynein [10,14]. Therefore, we next examined the interaction of importin β with dynein in the axotomized hippocampal neurons. Coimmunoprecipitation analysis revealed that importin β was associated with dynein and this association was increased 1 h after axotomy (Fig. 3I). These results suggest that importin β was increased in the axons in response to axotomy and that they interacted with the dynein motor complex for retrograde transport. We then investigated whether importin plays a role in inducing axonogenesis by employing Bimax, a peptide inhibitor of importin [15]. Our results showed that transfection of Bimax in the axotomized neurons efficiently blocked axonogenesis (Fig. 3J). Thus, the function of importin was found to be required for axotomy-induced axonogenesis.

4. Discussion

Reestablishment of axons after axotomy depends on the length of the remaining stump. Gomis-Rüth et al. reported that axotomy of the proximal part led to the transformation of a dendrite into an axon (identity change) [2], whereas axotomy of the distal part induced regrowth of the injured axon. As the distal axon is abundant in stable microtubules, this may enable microtubules to polymerize further at the process tip, leading to regrowth of the injured axon. However, when axotomized at a proximal site, the neuron loses the distal axon and its abundance of stable microtubules, and therefore, the neuron may not be able to make the injured axon regrow. Consistent with this observation, in our experimental model, axotomy at a proximal site induced a new axon to arise from the cell body or the transformation of a dendrite into an axon, whereas most of the axons severed at a distal site (>80 μm away from the cell body) regrew (data not shown).

In the present study, we characterized the previously unrecognized phenomenon of axotomy-induced axonogenesis in embryonic hippocampal neurons. It is not known how and why the proximally axotomized neuron chooses between the two responses: transformation of a dendrite into an axon or axonogenesis. Elucidation of the molecular mechanism underlining these responses may provide an answer. We assumed that some injury-induced signal might be transported with importin α/β heterodimers and dynein complex in the axotomized hippocampal neurons.

Our data suggest that retrograde axonal transport of the signals elicited by axonal injury is required for axonogenesis. We intended to inhibit retrograde axonal transport by overexpressing p50/dynamitin, as overexpression of p50 leads to disruption of dynactin [13,16]. However, it should be noted that overexpression of p50 inhibits not only retrograde axonal transport but also anterograde transport [17–19]. Dynactin is a motor protein coordinator whereby the opposing motors kinesin and dynein interact with dynactin, leading to vectorial transport. A direct interaction between $p150^{glued}$ and the anterograde motor kinesin-2 has also been demonstrated [17], and functional and biochemical interactions have been described for dynein and kinesin-1 [20]. Kwinter et al. [19] reported that bidirectional transport of dense-core vesicles was inhibited by overexpressing p50 in the axons and dendrites of primary cultured hippocampal neurons. Furthermore, dynactin has other functions in addition to axonal transport. Therefore, we should consider the possibility that overexpression of p50 attenuates axonogenesis by mechanisms other than inhibition of retrograde axonal transport. However, p50 overexpression did not affect neurite outgrowth, which is consistent with a previous report [21], suggesting a specific relationship between dynactin and axotomy-induced axonogenesis.

Acknowledgments

This work was supported by a Grant-in-Aid for Young Scientists (S) from JSPS.

References

[1] C.G. Dotti, G.A. Banker, Experimentally induced alteration in the polarity of developing neurons, Nature 330 (1987) 254–256.
[2] S. Gomis-Ruth, C.J. Wierenga, F. Bradke, Plasticity of polarization: changing dendrites into axons in neurons integrated in neuronal circuits, Curr. Biol. 18 (2008) 992–1000.
[3] E. Perlson, S. Hanz, K.F. Medzihradszky, A.L. Burlingame, M. Fainzilber, From snails to sciatic nerve: retrograde injury signaling from axon to soma in lesioned neurons, J. Neurobiol. 58 (2004) 287–294.
[4] P.M. Richardson, V.M. Issa, Peripheral injury enhances central regeneration of primary sensory neurones, Nature 309 (1984) 791–793.
[5] S. Neumann, C.J. Woolf, Regeneration of dorsal column fibers into and beyond the lesion site following adult spinal cord injury, Neuron 23 (1999) 83–91.
[6] X.P. Zhang, R.T. Ambron, Positive injury signals induce growth and prolong survival in aplysia neurons, J. Neurobiol. 45 (2000) 84–94.
[7] H. Wellmann, B. Kaltschmidt, C. Kaltschmidt, Retrograde transport of transcription factor NF-kappa B in living neurons, J. Biol. Chem. 276 (2001) 11821–11829.
[8] D. Gorlich, U. Kutay, Transport between the cell nucleus and the cytoplasm, Annu. Rev. Cell Dev. Biol. 15 (1999) 607–660.
[9] Y.M. Chook, G. Blobel, Karyopherins and nuclear import, Curr. Opin. Struct. Biol. 11 (2001) 703–715.
[10] S. Hanz, E. Perlson, D. Willis, J.Q. Zheng, R. Massarwa, J.J. Huerta, M. Koltzenburg, M. Kohler, J. van- Minnen, J.L. Twiss, M. Fainzilber, Axoplasmic importins enable retrograde injury signaling in lesioned nerve, Neuron 40 (2003) 1095–1104.
[11] S. Yamagishi, M. Fujitani, K. Hata, K. Kitajo, F. Mimura, H. Abe, T. Yamashita, Wallerian degeneration involves rho/rho-kinase signaling, J. Biol. Chem. 280 (2005) 20384–20388.
[12] T. Tanaka, M. Ueno, T. Yamashita, Engulfment of axon debris by microglia requires p38 MAPK activity, J. Biol. Chem. 284 (2009) 21626–21636.
[13] K.A. Melkonian, K.C. Maier, J.E. Godfrey, M. Rodgers, T.A. Schroer, Mechanism of dynamitin-mediated disruption of dynactin, J. Biol. Chem. 282 (2007) 19355–19364.
[14] E. Perlson, S. Hanz, K. Ben-Yaakov, Y. Segal-Ruder, R. Seger, M. Fainzilber, Vimentin-dependent spatial translocation of an activated MAP kinase in injured nerve, Neuron 45 (2005) 715–726.
[15] S. Kosugi, M. Hasebe, T. Entani, S. Takayama, M. Tomita, H. Yanagawa, Design of peptide inhibitors for the importin alpha/beta nuclear import pathway by activity-based profiling, Chem. Biol. 15 (2008) 940–949.
[16] K.C. Maier, J.E. Godfrey, C.J. Echeverri, F.K. Cheong, T.A. Schroer, Dynamitin mutagenesis reveals protein-protein interactions important for dynactin structure, Traffic 9 (2008) 481–491.
[17] S.W. Deacon, A.S. Serpinskaya, P.S. Vaughan, M. Lopez Fanarraga, I. Vernos, K.T. Vaughan, V.I. Gelfand, Dynactin is required for bidirectional organelle transport, J. Cell Biol. 160 (2003) 297–301.
[18] M. Haghnia, V. Cavalli, S.B. Shah, K. Schimmelpfeng, R. Brusch, G. Yang, C. Herrera, A. Pilling, L.S. Goldstein, Dynactin is required for coordinated bidirectional motility, but not for dynein membrane attachment, Mol. Biol. Cell 18 (2007) 2081–2089.
[19] D.M. Kwinter, K. Lo, P. Mafi, M.A. Silverman, Dynactin regulates bidirectional transport of dense-core vesicles in the axon and dendrites of cultured hippocampal neurons, Neuroscience 162 (2009) 1001–1010.
[20] L.A. Ligon, M. Tokito, J.M. Finklestein, F.E. Grossman, E.L. Holzbaur, A direct interaction between cytoplasmic dynein and kinesin I may coordinate motor activity, J. Biol. Chem. 279 (2004) 19201–19208.
[21] F.J. Ahmad, Y. He, K.A. Myers, T.P. Hasaka, F. Francis, M.M. Black, P.W. Baas, Effects of dynactin disruption and dynein depletion on axonal microtubules, Traffic 7 (2006) 524–537.

Clinical Neurophysiology 122 (2011) 2512–2517

Contents lists available at ScienceDirect

Clinical Neurophysiology

journal homepage: www.elsevier.com/locate/clinph

Activity-dependent changes in impulse conduction of single human motor axons: A stimulated single fiber electromyography study

Yu-ichi Noto [a,b,*], Sonoko Misawa [a], Kazuaki Kanai [a], Yasunori Sato [c], Kazumoto Shibuya [a], Sagiri Isose [a], Saiko Nasu [a], Yukari Sekiguchi [a], Yumi Fujimaki [a,d], Shigeki Ohmori [a], Masanori Nakagawa [b], Satoshi Kuwabara [a]

[a] Department of Neurology, Graduate School of Medicine, Chiba University, Chiba, Japan
[b] Department of Neurology, Graduate School of Medical Science, Kyoto Prefectural University of Medicine, Kyoto, Japan
[c] Clinical Research Center, Chiba University Hospital, Chiba, Japan
[d] Department of Neurology, Tokyo Metropolitan Neurological Hospital, Tokyo, Japan

ARTICLE INFO

Article history:
Accepted 4 May 2011
Available online 12 June 2011

Keywords:
Activity-dependent hyperpolarization
Activity-dependent conduction block
Single fiber electromyography
Single motor axon

HIGHLIGHTS

- In myelinated axons, trains of impulses activate electrogenic Na^+/K^+ pump and thereby axonal hyperpolarization.
- We developed a novel method to assess activity-dependent hyperpolarization in normal human motor axons.
- Single muscle action potentials recorded by single fiber EMG showed significant latency prolongation during tetanic stimulation.

ABSTRACT

Objective: The aim of this study is to develop a novel method to assess activity-dependent hyperpolarization in human single motor axons at a constant stimulus frequency by using intra-muscular axonal stimulating single fiber electromyography (s-SFEMG).
Methods: We performed s-SFEMG in the extensor digitorum communis (EDC) muscle of 10 normal subjects, and measured changes in latencies for single muscle fiber action potentials (MAPs) during 500 stimuli delivered at 5, 10 and 20 Hz. The data were analyzed with a repeated measurement analysis, and multiple comparisons were performed.
Results: A total of 585 MAPs were examined at 5 Hz ($n = 190$), 10 Hz ($n = 210$), and 20 Hz ($n = 185$) steady stimulation. There was a progressive linear prolongation of latencies, as the stimulus rate increased ($F = 95.6$, $p < 0.001$); the least square means (SEM) of latency change were 100.7 (0.28)% at 5 Hz, 102.3 (0.27)% at 10 Hz and 105.3 (0.28)% at 20 Hz. There were statistically significant differences between frequencies by Tukey–Kramer's method. Despite the significant latency prolongation, no activity-dependent conduction block developed. A 20 Hz electric stimulation to intramuscular axons was well-tolerated in all the subjects.
Conclusions: Tetanic stimulation at a constant rate results in significant latency increase in single human motor axons, the extent of which depends on the stimulus frequency. The findings imply that physiological discharge rates will activate the Na^+/K^+ pump and thereby produce axonal hyperpolarization in single motor axons.
Significance: This technique may detect activity-dependent conduction block if the safety margin of impulse transmission is significantly reduced by demyelination or increased branching due to collateral sprouting in a variety of neuromuscular disorders.

* Corresponding author at: Department of Neurology, Chiba University School of Medicine, 1-8-1 Inohana, Chuo-ku, Chiba 260-8670, Japan. Tel.: +81 43 222 7171x5414; fax: +81 43 226 2160.
E-mail address: y-noto@koto.kpu-m.ac.jp (Y.-i. Noto).

1388-2457/$36.00
doi:10.1016/j.clinph.2011.05.005

1. Introduction

Conduction of impulses, either individually or in trains, can produce long-lasting effects on nerve excitability. In 1935, Gasser found that when axons conducted trains of impulses, they underwent hyperpolarizaion (Gasser, 1935). Previous studies using high-frequency electrical stimulation for rat axons have shown that the phenomenon presumably occurs due to activity of the electrogenic Na^+–K^+ pump (Bostock and Grafe, 1985; Gordon et al., 1990). In a human motor axon, the extent and duration of hyperpolarization depend on both discharge rate and train length (Bostock and Bergman, 1994). Vagg et al. (1998) found that axonal hyperpolarization can be produced in human motor axons by the natural activity associated with a maximal voluntary contraction. It has recently been shown that voluntary contraction causes the change of other indices of axonal excitability (Kuwabara et al., 2001) and that the extent and pattern of axonal hyperpolarization could be measured by using threshold tracking technique (Kuwabara et al., 2002). Kiernan et al. (2004) clarified the axonal hyperpolarization in human median nerve by 8 Hz steady stimulation with surface electrodes. The reason why they used 8 Hz stimulation is because motor axons can maintain a tonic discharge at this frequency or even higher in voluntary contractions, and >10-Hz electric stimulation to the nerve trunk is painful and therefore not tolerable.

The safety margin for impulse conduction is normally high and the activity-dependent hyperpolarization induced by voluntary contraction is insufficient to jeopardize nerve conduction in healthy axons, but in demyelinated axons which have critical impairment of the safety margin, the conduction block can be induced by tetanic stimulation (Bostock and Grafe, 1985). The activity-dependent conduction block is potentially important in patients with demyelinating neuropathy such as chronic inflammatory demyelinating polyneuropathy and multifocal motor neuropathy. It has been reported that voluntary contraction produced (or accentuate) conduction block in patients with such demyelinating neuropathy (Cappelen-Smith et al., 2000; Kaji et al., 2000). In addition, Inglis et al. have shown by using microneurography that natural activity can produce conduction block in acutely injured single human axons (Inglis et al., 1998).

The single fiber electromyography (SFEMG) technique was developed to study the microphysiology of the motor unit, such as the propagation of muscle fibers (Stålberg, 1966) and neuromuscular jitter (Sanders and Stålberg, 1996). SFEMG recordings can be performed during intramuscular electrical stimulation. This stimulated SFEMG (s-SFEMG) technique can be used in patients who cannot cooperate (unconscious patients, children, and patients with very weak muscles) (Stålberg et al., 1992). The technique enables motor axons to fire at a constant frequency and provides the continuous data of latency from the time of the axonal stimulation to the onset of muscle-fiber action potential (MAP) including axonal conduction time. The continuous high frequency axonal stimulation during about 30 s may detect activity-dependent conduction block in patients with prominently reduced axonal safety factor because continuous high frequency stimulation could be equivalent to maximum voluntary muscle contractions. Moreover, when there are conduction blocks in the proximal nerves (e.g., the nerve roots), the impulse load at the more distal tested site at the nerve trunk should be less than expected, and it is impossible to estimate the extent of impulse load. In contrast by using the method of intramuscular axonal stimulation, it is possible to use a constant and steady impulse load. The present study has been undertaken to develop a method to assess activity-dependent hyperpolarization and block in single motor axons of human subjects by using s-SFEMG.

2. Methods

2.1. Subjects

Ten healthy subjects (5 males, 5 females; median age, 30 years; range, 20–50 years) were examined. None of them had a peripheral nerve disorder, and systematic disease or medication affecting peripheral nerve function. Informed consent was provided by each subject and all experiments were conducted in accordance with the *Declaration of Helsinki* and with the approval by the Ethics Committee of Chiba University School of Medicine for Human Research Studies.

2.2. Single fiber electromyography

Axonal s-SFEMG was performed in the right extensor digitorum communis muscle (EDC) using a Nicolet Viking 4 EMG machine (Nicolet Biomedical Japan, Tokyo, Japan) and conventional procedures as described in a previous report by Trontelj et al. (1986). The recordings were made intra-muscularly with a concentric needle electrode (30 G; TECA elite US53153). The high pass filter was set to 2 kHz, and the low pass filter was 10 kHz. Intra-muscular axonal stimulation was performed with a monopolar needle electrode (28 G; TECA U0809P02) and a reference surface electrode placed 2 cm laterally. The stimulus duration was 0.1 ms. With stimulating at 3 Hz with stimulus intensity around 1 mA, contraction of EDC was confirmed, and a recording electrode was inserted into the site of muscle bundle contraction. The distance between the stimulating and recording electrodes was 2 cm. Both needles were fixed by metallic strut to minimize needle moving during stimulation.

The stimulus intensity was determined as 20% above the activation threshold of the target MAP. The fingers of subjects were fixed with a strap to reduce motion artifacts. Although the muscle fibers can be stimulated either directly or indirectly via its axon in this s-SFEMG method, we excluded direct stimulation of muscle fibers by the very low jitter value (mean consecutive difference <5 μs) (Trontelj et al., 1986). By contrast, increased jitter with intermittent blocking indicates subthreshold stimulation. When it was observed, we performed a new recording 1 min later with increased stimulus intensity by further 20% of the previous intensity.

A total of 500 stimuli were delivered at the frequencies of 5, 10, and 20 Hz. Latencies of the initial rising phase of MAP were measured. A special program for latency measurements (Analysis of SFEMG software) was developed by Medical Try System Co. Ltd. (Tokyo, Japan). If a prominent latency change was observed after 500 times stimulation at 20 Hz, short time stimulation at the same frequency was repeated 1 min later to observe whether the latency prolongation was recovered or not.

2.3. Data analyses and statistics

Latency change (%) at 100th, 200th, 300th, 400th and 500th stimulus with each of the three stimulus rate was measured. Latency change was defined as "latency at 500th stimulation (or at 25 s after starting the stimulation)/latency at baseline × 100. We also calculated latency change at 25 s after the start of the stimulation with each stimulus rate (e.g., at 125th stimulus with 5 Hz stimulation, at 250th with 10 Hz and at 500th with 20 Hz) to compare the latency change at a constant time length.

The data of latency change were checked for normality using the Shapiro–Wilk test (Shapiro and Wilk, 1965) and Q–Q plot before using parametric tests. A repeated measurement analysis (Fitzmaurice et al., 2004) was conducted to evaluate the main effects of stimulation with the covariance among repeated measures

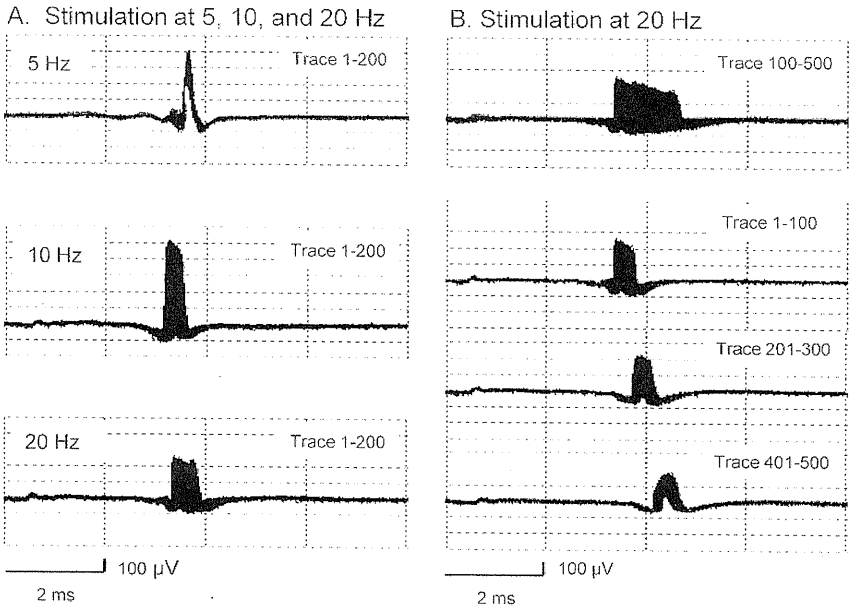

Fig. 1. Examples of superimposed single muscle action potentials during prolonged tetanic intramuscular microstimulation in the extensor digitorum communis muscle of a normal subject. (A) Characteristic responses during the first 200 stimuli delivered at 5, 10, and 20 Hz. Each superimposed response is recorded from a different site. (B) An example of superimposed responses recorded during 20 Hz stimulation. Traces 100–500, 1–100, 201–300, and 401–500 are separately shown. Note a progressive increase in latencies.

modeled as compound symmetry (CS). Tukey–Kramer's method (Westfall and Young, 1993) was applied for adjustment of multiple comparisons between any two groups. All comparisons were two-sided, and p-value of less than 0.05 was considered to be statistically significant. All statistical analyses were performed by the SAS software program, version 9.2 (SAS Institute Inc., Cary, NC, USA).

3. Results

A total of 585 MAPs were examined at 5 Hz ($n = 190$), 10 Hz ($n = 210$), and 20 Hz ($n = 185$) steady stimulation. The number of MAPs per subject were 12–27 at 5 Hz, 15–37 at 10 Hz and 12–27 at 20 Hz. The data of latency change (%) were analyzed for reducing the influence of latency at baseline determined by the distance between the stimulating electrode and the recording electrode. The tetanic electric stimulation was well-tolerated in all 10 subjects, whereas three of them complained of slight pain during 20 Hz stimulation.

There was a progressive linear prolongation of latencies, as the stimulus rate increased. Representative recordings from a single subject are shown in Fig. 1. The latency prolongation during stimulation was not observed at 5 Hz, but occurred slightly at 10 Hz, and prominently at 20 Hz. A gradual progressive latency prolongation was clearly visible at 20 Hz (Fig. 1B and Supplementary Video S1).

Fig. 2 shows changes in latency during 500 stimuli in two subjects. The baseline latencies varied because all three recordings in each subject were from different site to present characteristic examples. There were no obvious changes in latencies at 5 Hz, a slight increase in latency was seen at 10 Hz, and a clear latency prolongation at 20 Hz stimulation. The latency prolonged linearly and the slope of the regression line was steepest for 20 Hz stimulation. The slope of the formula of the regression line indicates the latency elongation (μs) per stimulus. In all recordings, the mean slope of the regression line was 0.07 μs/stimulus at 5 Hz, 0.26 μs/stimulus at 10 Hz and 0.53 μs/stimulus at 20 Hz.

Fig. 3 shows box plots of the latency change during 500 stimulations at 5, 10, and 20 Hz in the three different rate groups. The data of each stimulus rate group were normally distributed. There was a significant increase in latency, as the stimulus rate was increased. The least square means (SEM) of latency change by applying a mixed effect model were 100.7 (0.28)% at 5 Hz, 102.3 (0.27)% at 10 Hz and 105.3 (0.28)% at 20 Hz. The difference was more prominent between 10 and 20 Hz than between 5 and 10 Hz stimulation.

Fig. 4 shows comparison of latency change at constant time length, 25 s (125 stimuli at 5 Hz, 250 at 10 Hz, and 500 at 20 Hz). The data of three stimulus groups were also normally distributed. The least square means (SEM) of latency change were 100.2 (0.28)% at 5 Hz, 101.3 (0.28)% at 10 Hz and 105.3 (0.29)% at 20 Hz. Again there were statistically significant differences among three stimulus rate groups. During 500 stimuli, there was a linear chronological change in latency at 5, 10, and 20 Hz stimulation, and the latency increase was most prominent at 20 Hz (Fig. 5).

In most of recordings at 20 Hz stimulation in which we observed prominent latency prolongation, the same stimulation was repeated 1 min after the first trial. We confirmed the recovery from latency prolongation.

4. Discussion

The present study has demonstrated in healthy human motor axons, activity-dependent nerve conduction slowing by a constant frequency of prolonged electric stimulation, which presumably reflects activity-dependent hyperpolarization. The extent of impulse conduction slowing varied with stimulus rates. The method using axonal stimulation SFEMG appears to be able to assess the extent of activity-dependent hyperpolarization due to the activation of Na^+/K^+ pump in single motor axons. However, our method had some limitations. We could not demonstrate direct evidence that axonal membrane was hyperpolarized when the latency was prolonged (i.e., a threshold increase). Secondly, our study was on a small scale. To investigate the reliability of this method, further

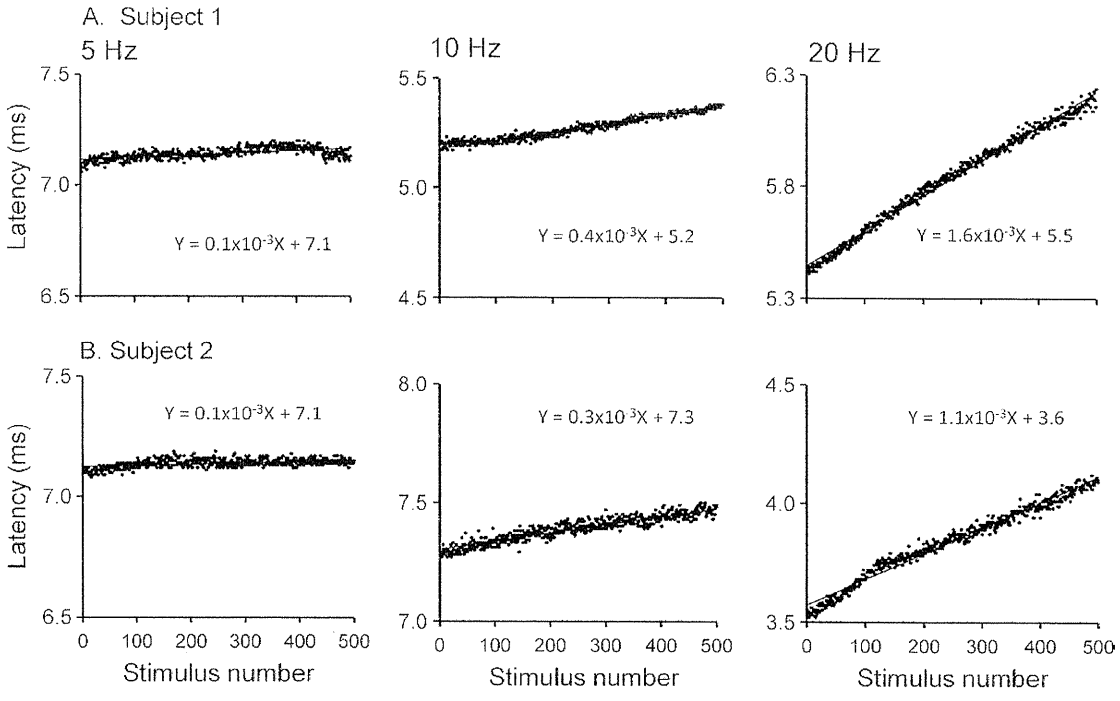

Fig. 2. Examples of the scatter plot of the latencies of single muscle action potentials at each stimulus rate recorded from different sites of two subjects. The equation of the linear function in each plot indicates the formula of the regression line. The slope of the formula represents the latency prolongation per stimulus. Note a progressive increase in latencies as the stimulus frequency increases.

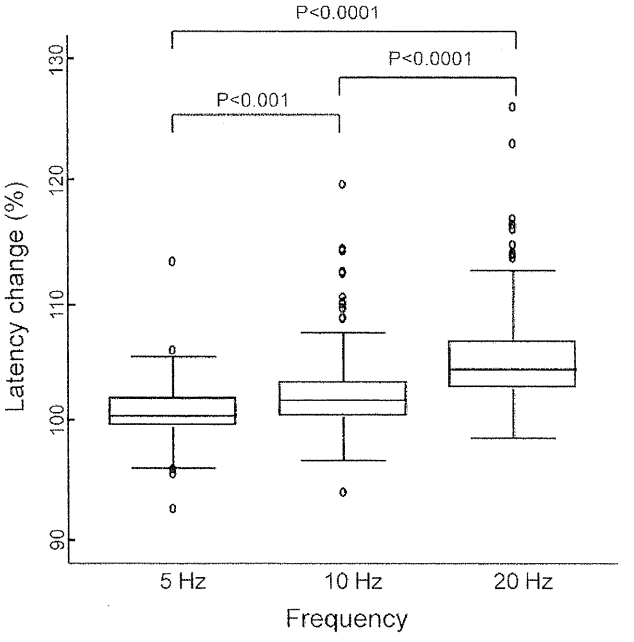

Fig. 3. Box plots of the latency change (%) at 500 times stimulation at 5 Hz ($n = 190$), 10 Hz ($n = 210$), and 20 Hz ($n = 185$). 5 Hz: median 100.6%; range 92.5–113.1% ; 10 Hz: median 101.7%; range 93.9–119.5%; 20 Hz: median 104.2%; range 98.5–125.9%. The data of latency change (%) are analyzed by means of repeated measurement analysis ($F = 95.6$, $p < 0.001$) and multiple comparisons are calculated by means of Tukey–Kramer's method. There are statistically significant differences among latency changes among each frequency (p-values are given in the figure).

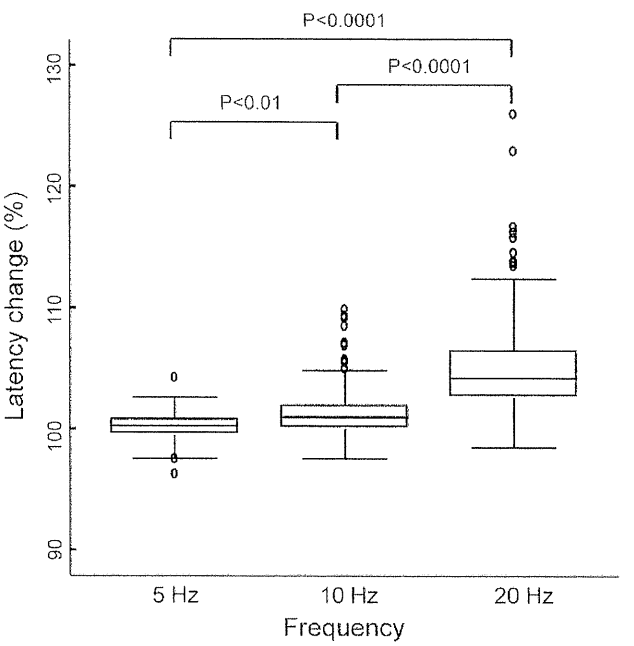

Fig. 4. Box plots of the latency change (%) during a constant stimulus length (25 s). 5 Hz: median 100.3%; range 96.2–104.2% ; 10 Hz: median 101.0%; range 97.6–109.8%; 20 Hz: median 104.2%; range 98.5–125.9%. The data of latency change (%) are analyzed by means of repeated measurement analysis ($F = 196.8$, $p < 0.001$) and multiple comparisons are calculated by means of Tukey–Kramer's method. There are statistically significant differences between frequencies (p-values are given in the figure).

studies involving a larger number of subjects or other population will be required.

Particularly, prolonged repetitive stimulation at 20 Hz results in obvious latency prolongation of MAPs. In most part of recordings with obvious latency prolongation, we observed slightly decreasing amplitude and increasing duration of the action potential as the latency prolonged (Supplementary Video S1). The change of

the amplitude and duration of action potential might be due to slowing of the propagation velocity of the muscle fiber action potential by continuous activation.

4.1. Mechanisms of the activity-dependent latency prolongation

Along with previous studies, the latency increases are supposed to be induced by activation of the electrogenic Na^+/K^+ pump and resulting axonal hyperpolarization (Vagg et al., 1998; Kuwabara et al., 2001, 2002). Two major mechanisms could be responsible for the hyperpolarization that follows activity; activation of slow potassium channels and activation of the electrogenic Na^+/K^+ pump.

It has been reported that with trains of 10–20 impulses, slow potassium channels can be a main mechanism for axonal hyperpolarization, and more prolonged impulse trains cause activation of the electrogenic Na^+/K^+ pump and thereby axonal hyperpolarization (Bergman, 1970; Lin et al., 2000). It is therefore likely that trains of 500 impulses used in this study result in activation of the pump. The latency reflects axonal conduction time, neuromuscular junction transmission time and muscle fiber conduction time. The neuromuscular transmission is established by presynaptic acetylcholine release, and the intervals of the release are random, not steady. Scatter plots of all recordings in this study could apply to linear models, and the mean slope of the regression line was steeper, as stimulus frequency increased.

The linear prolongation of the latency is likely to reflect prolongation of axonal conduction time due to membrane hyperpolarization, although the possibility that changes in muscle membrane properties may partly contribute to the observed latency changes during tetanic stimulation, could not be excluded. This is a limitation of our method, and further studies are required to clarify the precise mechanisms for the activity-dependent changes.

4.2. The advantage of the s-SFEMG method

Our s-SFEMG method could provide quantitative assessment in single motor axons because axons can be activated at a fixed frequency. In a previous study by Kiernan et al. (2004), axonal stimulation has been demonstrated by 8 Hz surface electrode stimulation at the wrist (Kiernan et al., 2004). It has been noted that higher frequency stimulation over 8 Hz was more painful and this made it more difficult for naïve volunteers to relax in their study. However, high frequency stimulation over 10 Hz is available by the s-SFEMG method without pain. In steady voluntary contractions, motor axons discharge at 6–20 Hz (Burke and Jankelowitz, 2009). Therefore 20 Hz stimulation is more equivalent to physiological maximum voluntary contraction than 8 Hz stimulation.

4.3. Clinical implications

The present study shows that the s-SFEMG method could be used to assess the degree of membrane hyperpolarization in normal human motor axons. The procedure is easy and safe, and therefore can be applied to patients with neuromuscular disorder, particularly who complained of fatigability. Activity-dependent conduction block could be responsible for fatigue in patients with demyelinating neuropathy, such as chronic inflammatory demyelinating polyneuropathy (Burke and Jankelowitz, 2009).

In normal axons, the activity-dependent hyperpolarization causes nerve conduction slowing, but does not cause conduction block because of the sufficiently high safety margin for impulse transmission at each node. By contrast, previous studies have demonstrated that activity-dependent conduction block occurred in demyelinated axons in rat and patients with demyelinating neuropathy (Bostock and Grafe, 1985; Kaji et al., 2000; Cappelen-Smith et al., 2000). We speculate that patients with a number of diseases in which the safety factor for impulse transmission is critically lowered by not only demyelination but also increased axonal branching due to collateral sprouting suffer from fatigability due to activity-dependent conduction block. Our technique by using 20 Hz stimulation may detect activity-dependent conduction block if the safety margin of impulse transmission is reduced, and would provide the mechanism for fatigue in disease.

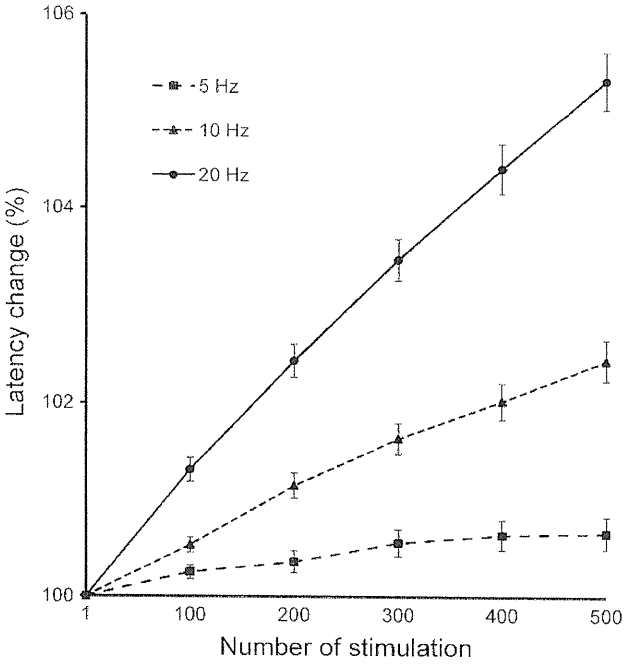

Fig. 5. Change in the mean latency prolongation at 5, 10, and 20 Hz stimulation. There was a linear trend in the chronological changes in the rate of the latency prolongation at each stimulus rate, and the slopes become steeper as the stimulus frequency is increased.

Acknowledgements

This work was supported by Grants-in-Aid from the Research Committee of CNS Degenerative Diseases (M.N. and S.K.), and of Intractable Diseases (Neuroimmunological Diseases), the Ministry of Health, Labour and Welfare of Japan (M.N. and S.K.).

Appendix A. Supplementary data

Supplementary data associated with this article can be found, in the online version, at doi:10.1016/j.clinph.2011.05.005.

References

Bergman J. Characteristics of post-tetanic hyperpolarisation of a bundle of myelinizated nervous fibers. C R Seances Soc Biol Fil 1970;164:1254–61.
Bostock H, Grafe P. Activity-dependent excitability changes in normal and demyelinated rat spinal root axons. J Physiol 1985;365:239–57.
Bostock H, Bergman J. Post-tetanic excitability changes and ectopic discharges in a human motor axon. Brain 1994;117:913–28.
Burke D, Jankelowitz SK. Fatigue in chronic inflammatory demyelinating polyneuropathy. Muscle Nerve 2009;39:713–4.
Cappelen-Smith C, Kuwabara S, Lin CS, Mogyoros I, Burke D. Activity-dependent hyperpolarization and conduction block in chronic inflammatory demyelinating polyneuropathy. Ann Neurol 2000;48:826–32.
Fitzmaurice GM, Laird NM, Ware JH. Applied longitudinal analysis. New York: Wiley; 2004.